The Dynamics of Solitons

Gerry O'Brien

***Abstract*— The aim of this project was to investigate soliton dynamics using numerical methods to solve the Korteweg de Vries equation, Inviscid Burgers equation, and Burgers equation. The focus was on soliton collisions, wave breaking, and shock waves and these aspects have been observed and analysed.**

I. INTRODUCTION

Solitons are solitary waves that maintain a constant shape and speed whist propagating and remain unchanged by collisions. They are solutions to select non-linear partial differential equations such as the 'Inviscid Burger's equation' and the 'Korteweg de Vries (KdeV) equation' which is investigated numerically in this project [1].

Solitons have been key in the development of many methods for solving non-linear partial differential equations. They have been used in fiber optics, where the concept has been employed in long distance signal transmission, and biology, where soliton theory has been used to further understand energy propagation in bio-membranes and nerves [1].

The KdeV partial differential equation is shown in equation (1),

$$\frac{\partial u}{\partial t} + u\frac{\partial u}{\partial x} + \frac{\partial^3 u}{\partial x^3} = 0 \quad (1)$$

and has analytical solutions given by equation (2),

$$u = 12\alpha^2 sech^2(\alpha(x - 4\alpha^2 t)) \quad (2)$$

where α is an adjustable parameter. From equation (1), the second non-linear term describes a wave speed which is dependent on soliton amplitude and the third term describes dispersive broadening of the wave as it propagates. These effects 'cancel each other out exactly' to allow the solitons to propagate without a change of shape [2].

II. NUMERICAL METHODS

To investigate the dynamics of solitons, first a numerical method needs to be applied to solve the equation for an input wave.

The first step is discretising the spatial derivatives which was done using central difference approximations. The last two terms in equation (1) become,

$$u\frac{\partial u}{\partial x} = \frac{1}{4h}[(u_{i+1}^n)^2 - (u_{i-1}^n)^2] \quad (3)$$

$$\frac{\partial^3 u}{\partial x^3} = \frac{1}{2h^3}[u_{i+2}^n - 2u_{i+1}^n + 2u_{i-1}^n - u_{i-2}^n] \quad (4)$$

where h is the spatial step, the subscript 'i' describes the spatial position, and the superscript 'n' describes the temporal position. A derivation of these results can be found in Appendix 1.

The next step is choosing a method to solve the time derivative. The Euler Method was deemed to lead to instability of this difference scheme, with an analytical proof shown in Appendix 2. A second-order Runge-Kutta Method was attempted but gave solutions quite varied from the analytical solution after a small number of time steps. The method used is the fourth-order Runge-Kutta of the form described by the equations below.

$$f_a = f(t^n, u^n)$$

$$f_b = f(t^n + \frac{\Delta t}{2}, u^n + \frac{f_a \Delta t}{2})$$

$$f_c = f(t^n + \frac{\Delta t}{2}, u^n + \frac{f_b \Delta t}{2})$$

$$f_d = f(t^n + \Delta t, u^n + f_c \Delta t)$$

$$u^{n+1} = u^n + \frac{1}{6}(f_a + 2f_b + 2f_c + f_d)\Delta t \quad (5)$$

where Δt is the time step and the function 'f' is $\frac{\partial u}{\partial t}$. I could use periodic boundary conditions as I ensured the total spatial extent considered is large in comparison to the pulse width. This condition suggests the space domain is effectively infinite, as the front of the soliton can't affect the back.

III. VALIDATION

To validate the KdeV solver I compared the numerical solutions to the analytical solutions for a range of α, ensuring that the soliton could propagate for at least a few timesteps without varying too far from the analytical solution. To do this I used an initial input of the analytical solution, equation (2), at t=0s.

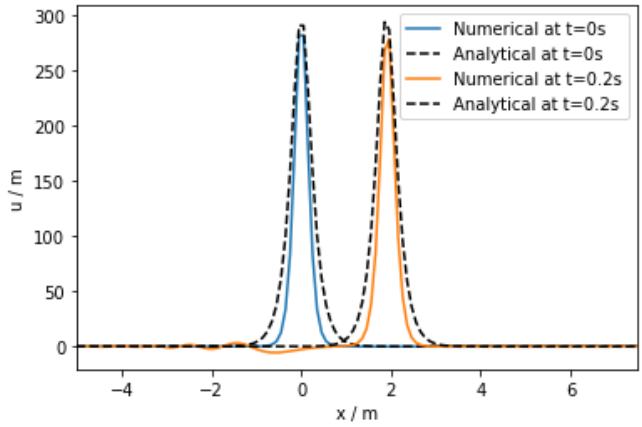

Figure 1 - A plot comparing the numerical and analytical solutions at t=0s and t=0.2s, α=5, Δt = 0.001s, h=0.1m.

Figure 1 shows how the numerical solution propagates in time and how it compares to the analytical solution. Overall, the numerical solutions are very similar to the analytical solutions. The analytical solutions are solitons with a slightly wider spread, and larger height, than the numerical solutions. Whilst this is not ideal, I decided that the error here was okay as it remains relatively constant over a range of time steps, and α values, allowing me to measure and analyse any effects under consideration. Similar plots for α = 2.5, 7.5 can be found in Appendix 3. At higher values of α the numerical solution starts to lag behind the analytical solution due to a slightly lower propagation speed. For all α tested the soliton propagates with no significant change in shape.

The numerical solution has an oscillating left tail, with the amplitude of the oscillations initially increasing in time. This is due to the third dispersive term of the KdeV which serves to prevent discontinuities from forming in the solution [3]. This might be resolved by re-weighting the central difference scheme in favour of the second term in the KdeV equation.

From the analytical solution, the height of the soliton is $12\alpha^2$m and the propagation speed is $4\alpha^3$m/s. This gives the relationship shown in equation (6),

$$Height = \frac{3}{\alpha} Speed \quad (6)$$

which has been confirmed for the numerical solutions.

The final step of validation is investigating the values of h and Δt needed for stability for different values of α. I chose a value of h = 0.1m because, with a larger h, the soliton has a very discontinuous shape, introducing larger inaccuracies ($O(h^2)$) and making comparisons to analytical solutions very difficult. With a smaller h = 0.01m, the solver became unstable for all Δt greater than 0.00001s. Upon choosing these values of h and Δt, the soliton propagates very slowly with respect to code runtime, making this an inefficient option in the context of this project.

Using the chosen h = 0.1m, I investigated the instability of different Δt values on solitons of different α values, plotting the difference between numerical and analytical solutions over 20 timesteps. An example of this plot for α = 6 is shown in figure 2 with the same plot for different α values shown in Appendix 4.

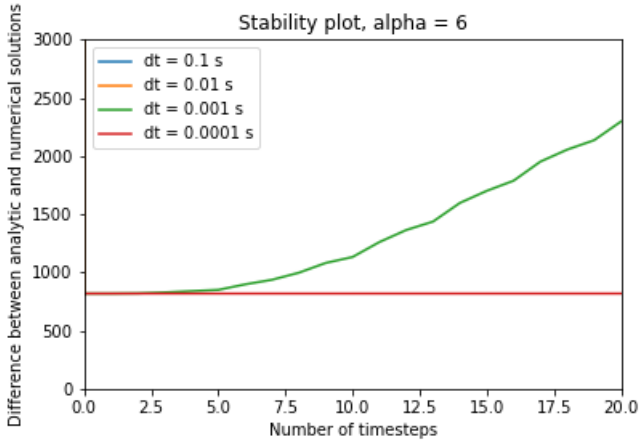

Figure 2 - The difference between analytical and numerical solutions, summed over the full x domain, across 20 time steps, for α=6. 'dt' is equivalent to Δt.

In general, as you increase α the difference between the analytical and numerical solutions increases. For all values of α between 1 and 10, the Δt = 0.1s and Δt = 0.01s solutions are unstable within the first two time steps, hence aren't visible on most of the plots. Up to about α = 4, both Δt = 0.001s and Δt = 0.0001s remain stable over the first 20 time steps. For higher α values (up to a limit of 10) Δt = 0.0001s is the only one that remains relatively stable over 20 time steps so this is the Δt selected when investigating solitons with α > 5 or other input wave forms.

IV. Collisions of Solitons

To investigate the collision of solitons in one dimension, I looked at two cases: two solitons with very different speeds and amplitudes, and two solitons of similar speeds and amplitudes.

The first case collision is shown in figure 3 at a range of different times.

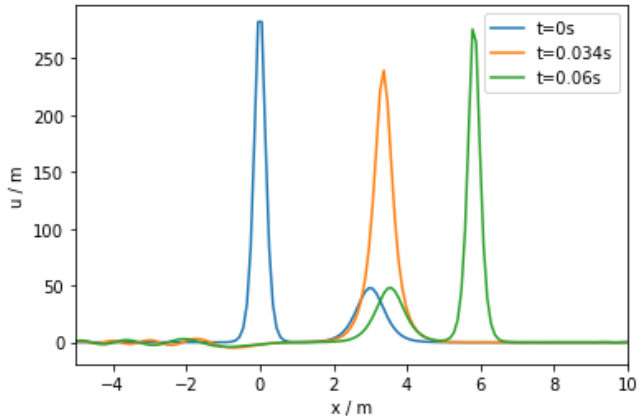

Figure 3 - A plot showing the interaction between two solitons of α=5 and α=2.

The input wave, at t=0s, is an α=5 soliton behind an α=2 soliton. The collision begins at about 0.02s as the faster soliton starts to overtake the slower one. The amplitude of the faster soliton decreases according to figure 4.

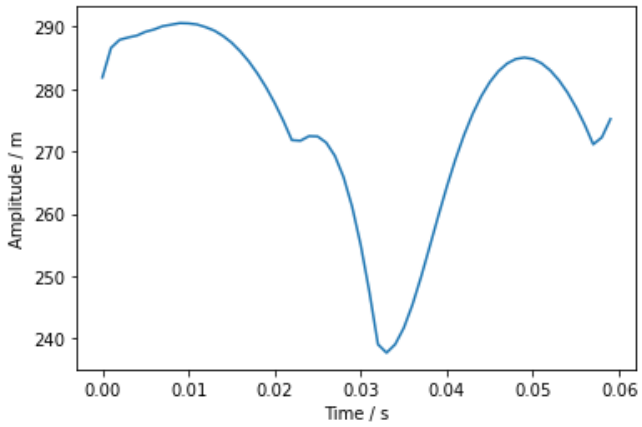

Figure 4 - A plot of α=5 soliton amplitude against time during the collision with the α=2 soliton.

Whilst there are changes in amplitude outside of the collision, due to errors in the central difference scheme, the maximum decrease in amplitude of the faster soliton is approximately equal to the initial amplitude of the slower soliton (48m).

At t = 0.034s, in figure 3, the solitons are mid-way through their collision and the faster soliton has effectively engulfed the slower one, getting wider with less amplitude. At t = 0.06s, both solitons have returned to their original shape with the faster one now in front of the slower one. Their speeds remain constant throughout.

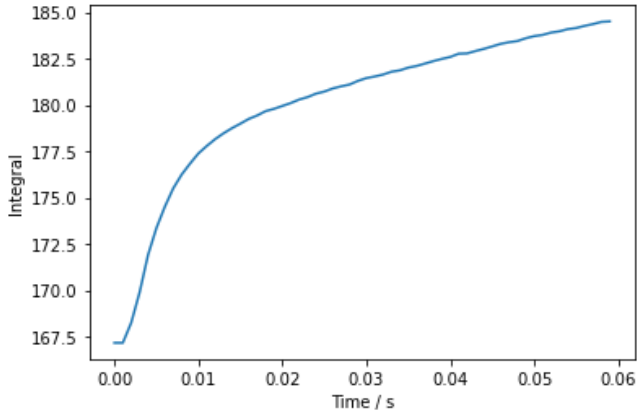

Figure 5 - A plot of the integral across the total spatial domain throughout the α=5 and α=2 soliton collision.

The quantity expected to be conserved throughout the collision is the integral across the spatial domain. Figure 5 shows how the integral changes throughout the collision. The integral was calculated using the trapezoidal rule. There is a log(t) style increase over time due to the formation of the smaller wavelength oscillations to the left of the solitons, which increase linearly in amplitude initially and then approach a constant value and by inspection appears to happen at around t = 0.07s. There is no indication of the collision itself affecting the integral as we would see a different function appear around collision time (0.02s).

The second case collision is shown in figure 6 at a range of different times.

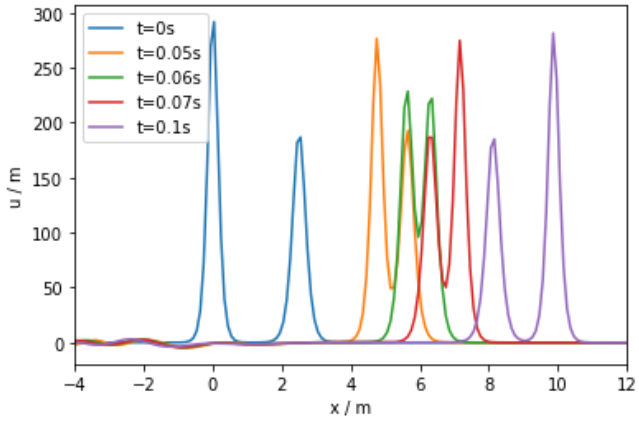

Figure 6 - A plot showing the interaction between two solitons of α=5 and α=4.

This time the input wave is an α=5 soliton behind an α=4 soliton. The solitons start to interact at around t=0.05s and at t=0.06s the solitons are observed to both decrease in amplitude, in contradiction to what would happen if the two pulses overlapped linearly. They then appear to exchange amplitude and velocity, as expected for two solitons of similar amplitudes [3]. This suggests the collision is an elastic one.

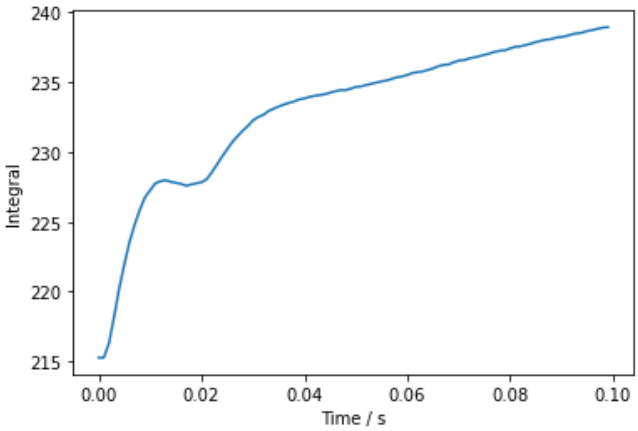

Figure 7 - A plot of the integral across the total spatial domain throughout the α=5 and α=4 soliton collision.

Again, looking at figure 7, the integral across the total spatial domain, is unaffected by the collision itself. It shows a similar function to figure 6 with a dip at around t=0.02s which is just before the collision begins, suggesting this is a result of the central difference scheme inaccuracy or that of the trapezoidal rule integration.

V. Wave Breaking

Solutions of the form of equation (2) can be considered normal modes of the KdeV equation [2]. It is expected that waves not of this form should break up into solitons of different amplitudes and speeds.

This effect can be described in three time intervals. Initially the first two terms of the KdeV equation dominate the propagation, causing the wave to steepen in places with a negative gradient as parts of the wave with a larger amplitude travel faster. Then the third term starts to work to prevent any discontinuity formation. Small wavelength oscillations to the left of the wave grow in amplitude until steady amplitude almost-solitons are formed. These amplitudes should increase linearly from left to right. Finally, the solitons spread out as they propagate with speeds linearly proportional to their height, according to equation (6). [3]

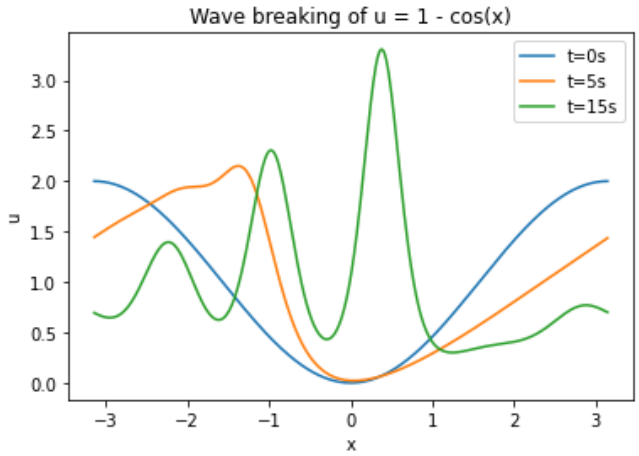

Figure 8 - Wave breaking of a cosine wave. u is in [m], x is in [m].

Figure 8 shows the expected wave breaking for a cosine input wave with the three time intervals aforementioned plotted. To see this effect it is important to ensure the period of the input wave is large relative to its amplitude.

Figure 9 shows the wave breaking of a sech function as it is put through the KdeV solver.

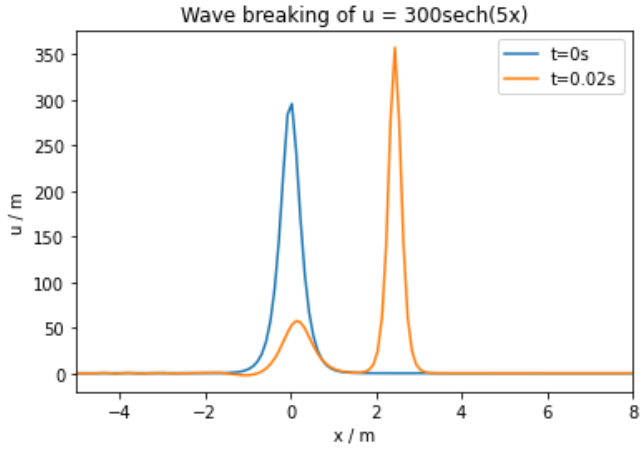

Figure 9 - Wave breaking of a sech function.

The sech function breaks up into two solitons of $\alpha \approx 5.4$ and $\alpha \approx 2.1$ with the larger amplitude soliton propagating faster to the right than the smaller amplitude soliton.

VI. Shock Waves

If you remove the third dispersive term from the KdeV equation, you lose the balance with the non-linear term, leaving a wave equation for a type of shockwave. This is known as the Inviscid Burgers equation [4].

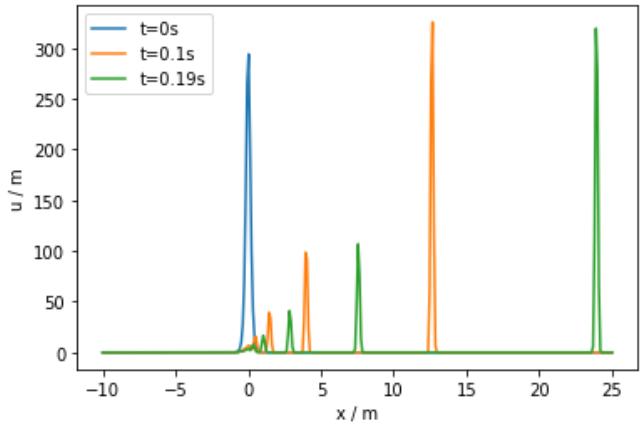

Figure 10 - The propagation of shock waves when equation (2) is used as an input wave in the Inviscid Burgers equation.

Figure 10 shows the formation and propagation of shock waves when equation (2) is used as the input wave in the Inviscid Burgers equation solver. Within the first 0.03s three distinct shock waves have formed at their constant amplitudes. The largest amplitude waves form first and propagate at the fastest speeds, creating a spacing between each wave which increases with time.

I ran the modified solver, with the same input wave, for a larger number of timesteps, of the order 50000, and found that the solution becomes unstable after about 35000 time steps (3.5s). This is due to the peaks of the shock waves overtaking their bases creating non unique values for a given value of x, and discontinuities causing the solver to break down [4]. Hence, I introduced a diffusive term making the Burgers equation, shown in equation (7),

$$\frac{\partial u}{\partial t} + u\frac{\partial u}{\partial x} - D\frac{\partial^2 u}{\partial x^2} = 0 \quad (7)$$

where D is the diffusion coefficient. I used a forward difference scheme to discretise the new second spatial derivative according to equation (8), with an error of $O(h^2)$.

$$D\frac{\partial^2 u}{\partial x^2} = D\frac{D}{h^2}(u_{i-1}^n - 2u_i^n + u_{i+1}^n) \quad (8)$$

The introduction of this term solved the instability issue by suppressing any wave breaking and discontinuity formation, as expected [6]. Through trial and error, I deduced that $0 < D < 1$ is needed for the shock waves to propagate with a relatively constant shape.

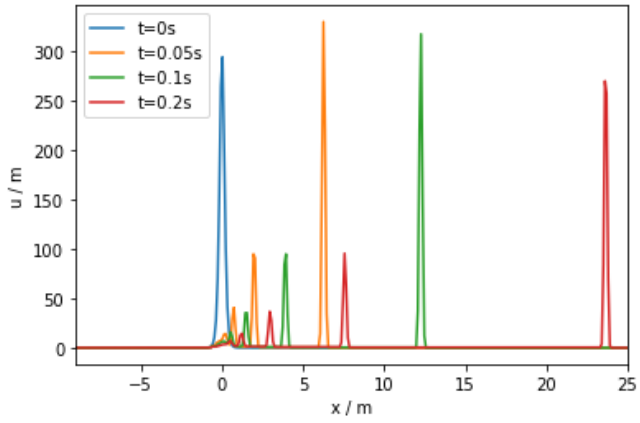

Figure 11 - The propagation of shock waves when a diffusive term is introduced for D=0.01.

Figure 11 shows the propagation of shock waves when the diffusive term, equation (7), is included in the solver, for D = 0.01. Comparing to figure 10, the diffusive term causes the shock waves to lose amplitude as they propagate. Furthermore, the smaller the diffusive term, the faster the shock waves propagate. As D tends to zero, the solution approaches that of the Inviscid Burgers equation, as expected [4].

VII. Conclusion

In conclusion, I built a successful numerical KdeV solver and used it to effectively observe and analyse the effects at play during 1-dimensional soliton collisions and wave breaking into soliton normal modes.

Given more time, I would attempt to further understand the formation and propagation of shock waves by investigating the agreement between small D and the theory of scalar conservation laws [5]. I would also focus on trying to understand exactly what is happening just before the Inviscid Burgers equation solution becomes unstable.

VIII. References

[1] S. Manukure et al. (2021) A short overview of solitons and applications. *Partial Differential Equations in Applied Mathematics*. 4 (100140)

[2] M. Scott and P. Dauncey (2022) Project 3: *The Dynamics of Solitons*. Computational Physics 2022-23. Imperial College London

[3] N.J. Zabusky and M.D. Kruskal (1965) Phys. Rev. Lett. 15, 240-243

[4] M. Landajuela (2011) Burgers Equation. *Basque centre for applied mathematics.* BCSM Internship.

[5] N.a. (n.d.) *The Burgers equation*. chrome-extension://efaidnbmnnnibpcajpcglclefindmkaj/htt

ps://math.nyu.edu/~tabak/PDEs/The_Burgers-Equation.pdf [Accessed 13th December 2022]
[6] A. Salih (2016) *Burgers' Equation*. Department of Aerospace Engineering, Indian Institute of Space Science and Technology

IX. Appendix

1. Discretisation derivation:

$$u_{i+1} = u_i + \frac{du}{dx}h + \frac{1}{2}\frac{d^2u}{dx^2}h^2 + \frac{1}{3}\frac{d^3u}{dx^2}h^3 + O(h^5)$$

$$u_{i-1} = u_i - \frac{du}{dx}h + \frac{1}{2}\frac{d^2u}{dx^2}h^2 - \frac{1}{3}\frac{d^3u}{dx^2}h^3 + O(h^5)$$

$$u_{i+2} = u_i + \frac{du}{dx}(2h) + \frac{1}{2}\frac{d^2u}{dx^2}(2h)^2 + \frac{1}{3}\frac{d^3u}{dx^2}(2h)^3 + O(h^5)$$

$$u_{i-2} = u_i - \frac{du}{dx}(2h) + \frac{1}{2}\frac{d^2u}{dx^2}(2h)^2 - \frac{1}{3}\frac{d^3u}{dx^2}(2h)^3 + O(h^5)$$

For $u\frac{\partial u}{\partial x}$:

$$(u_{i+1})^2 - (u_{i-1})^2 = 4hu\frac{du}{dx} + O(h^3)$$

For $\frac{\partial^3 u}{\partial x^3}$:

$$(u_{i+2} - u_{i-2}) - 2(u_{i+1} - u_{i-1}) = 2h^3\frac{d^3u}{dx^3} + O(h^5)$$

2. Euler Method Instability:
Using the von Neumann stability analysis method

$$u_i^{n+1} = gu_i^n \quad (1)$$
$$u_{i+1}^n = u_i^n e^{ikh} \quad (2)$$
$$u_{i+2}^n = u_i^n e^{2ikh} \quad (3)$$
$$u_i^{n+1} = u_i^n + \frac{\partial u}{\partial t}\Delta t \quad (4)$$

Inputting (1),(2),(3) as well as $\frac{\partial u}{\partial t}$ = - central difference approximation, in the limit of small u, into (4),

$g = 1 - a(e^{2ikh} - 2e^{ikh} + 2e^{-ikh} - e^{-2ikh})$
where $a = \frac{\Delta t}{2h^3}$.
$|g|^2 = 1 + a^2(2\sin(2kh) - 4\sin(kh))^2 \geq 1$

3. Comparing numerical and analytical solutions for different α values:

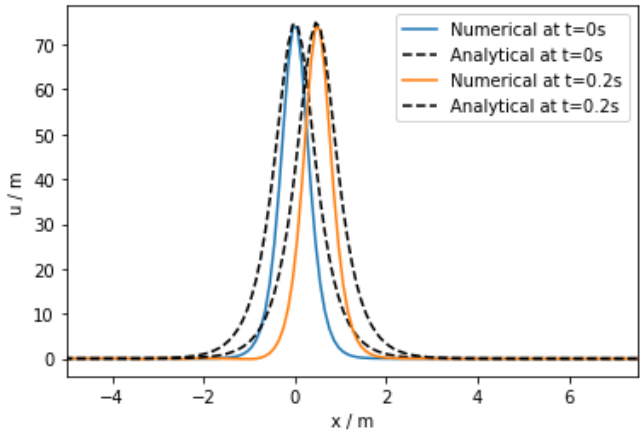

Figure 12 - A plot comparing the numerical and analytical solutions at t=0s and t=0.2s, α=2.5, Δt = 0.001s, h=0.1m.

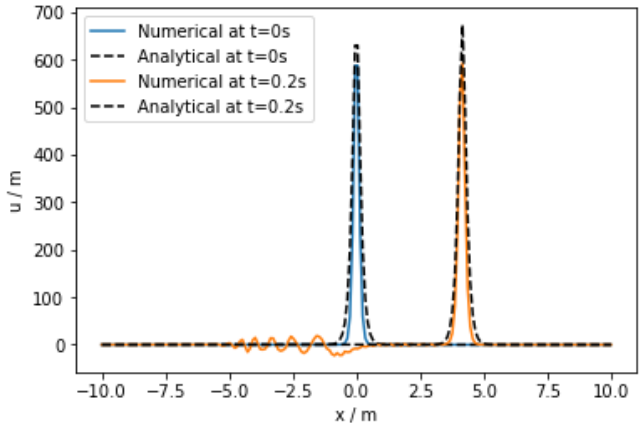

Figure 13 - A plot comparing the numerical and analytical solutions at t=0s and t=0.2s, α=7.5, Δt = 0.0001s, h=0.1m.

4. Stability plots for a range of Δt values with h=0.1m, α=7:

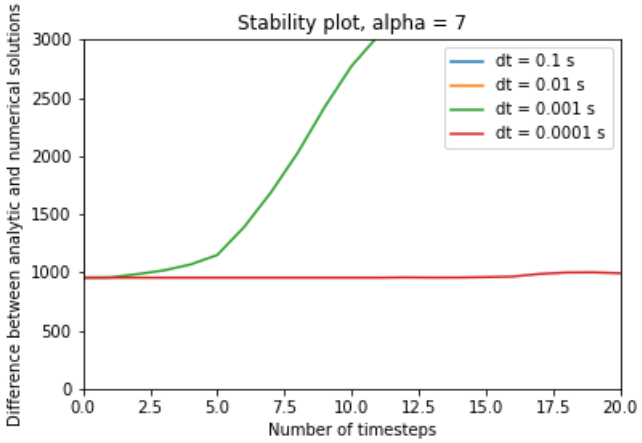

Figure 15 - The difference between analytical and numerical solutions, summed over the full x domain, across 20 time steps, for α=7. 'dt' is equivalent to Δt.